



1 **Significant submarine ice loss from the Getz Ice Shelf, Antarctica**

2 **David M. Rippin**

3 *Department of Environment and Geography, University of York Wentworth Way, Heslington, York,*
4 *YO10 5NG.*

5 **1. Abstract**

6 We present the first direct measurements of changes taking place at the base of the Getz Ice Shelf
7 (GzIS) in West Antarctica. Our analysis is based on repeated airborne radio-echo sounding (RES)
8 survey lines gathered in 2010 and 2014. We reveal that while there is significant variability in ice
9 shelf behaviour, the vast majority of the ice shelf (where data is available) is undergoing basal
10 thinning at a mean rate of nearly 13 m a^{-1} , which is several times greater than recent modelling
11 estimates. In regions of faster flowing ice close to where ice streams and outlet glaciers join the ice
12 shelf, significantly greater rates of mass loss occurred. Since thinning is more pronounced close to
13 faster-flowing ice, we propose that dynamic thinning processes may also contribute to mass loss
14 here. Intricate sub-ice circulation patterns exist beneath the GzIS because of its complex sub-ice
15 topography and the fact that it is fed by numerous ice streams and outlet glaciers. It is this
16 complexity which we suggest is also responsible for the spatially variable patterns of ice-shelf change
17 that we observe. The large changes observed here are also important when considering the
18 likelihood and timing of any potential future collapse of the ice shelf, and the impact this would have
19 on the flow rates of feeder ice streams and glaciers, that transmit ice from inland Antarctica to the
20 coast. We propose that as the ice shelf continues to thin in response to warming ocean waters and
21 climate, the response of the ice shelf will be spatially diverse. Given that these measurements
22 represent changes that are significantly greater than modelling outputs, it is also clear that we still
23 do not fully understand how ice shelves respond to warming ocean waters. As a result, ongoing
24 direct measurements of ice shelf change are vital for understanding the future response of ice
25 shelves under a warming climate.

26

27 **2. Introduction**

28 Warming ocean waters are a recognised consequence of global warming trends, and ice shelves
29 which float in these warming waters are prone to significant melting activity. This is important
30 because ice shelves are an interface between grounded ice and the oceans and are therefore sites
31 where these key interactions occur (Berger *et al.*, 2017). For example, past work has shown that
32 many of the ice shelves found along the Antarctic Peninsula have, in recent years, undergone
33 significant and rapid retreat, and in some cases collapse (e.g. Rott *et al.*, 1998; Holt *et al.*, 2013).
34 There is evidence of a gradual southwards progression of these occurrences, suggesting that there is
35 an underlying climatic cause (Schannwell, 2018). Such changes are significant because ice shelves
36 have a crucial role to play in regulating the rate of grounded ice-loss to the oceans (e.g. Scambos *et al.*,
37 2000, 2004; Dupont and Alley, 2005; Pritchard *et al.*, 2012; De Rydt *et al.*, 2015). Although the
38 mechanisms behind these changes are complex, any thinning enhanced by basal melting is caused
39 by variations in oceanic temperature and ocean circulation due to oceanic warming (e.g. Pritchard *et al.*,
40 2012).



41 Of the order of 74% of Antarctica is bounded by these floating ice shelves (Blindschadler *et al.*, 2011;
42 Berger *et al.*, 2017), and the Getz Ice Shelf (GzIS) is one of many regions of floating ice around the
43 Antarctic Peninsula. It is approximately 650 km in length and covers an area of approximately 33,395
44 km², occupying a portion of the Antarctic perimeter in the Amundsen Sea (Jacobs *et al.*, 2013; Rignot
45 *et al.*, 2013). A recent modelling study also showed that of all the Antarctic ice shelves, it is those of
46 the Amundsen Sea (including the GzIS) where greatest changes are forecast to happen in the
47 decades to come, as a result of warming ocean waters (Naughten *et al.*, 2018). Understanding the
48 changes going on here are thus of great importance, and arguably greater importance than
49 elsewhere. Amongst Antarctic ice shelves, the GzIS is unique because its large size and position
50 means that it is exposed to a more varied ocean environment than other ice shelves (Jacobs *et al.*,
51 2013). It also differs from other ice shelves because it is fed by numerous glaciers and ice-streams.
52 Furthermore, it is characterised by a margin which is anchored by many small islands and inland
53 grounded regions, and it is thought that these might have an impact on calving rates and on
54 circulation of ocean waters in sub-ice cavities (e.g. Rignot *et al.*, 2011; Jacobs *et al.*, 2013). Previous
55 work has suggested that Circumpolar Deep Water (CDW) beneath the GzIS may actually be cooler
56 than that found elsewhere (Jacobs and Giulivi, 2010; Jacobs *et al.*, 2012; Jacobs *et al.*, 2013), and
57 combined with the sheer size of the GzIS and its complex ocean-boundary, there may be highly
58 variable rates of submarine melting here. Despite these suggestions, in reality, relatively little is
59 known about general rates of submarine melting beneath floating ice-shelves (Horne *et al.*, 1985;
60 Walters *et al.*, 1988; Motyka *et al.*, 2003), let alone the nature of such complexity which may exist
61 here in the GzIS. Wilson and Straneo (2015) do suggest that where ice tongues are thickest, and
62 where ocean waters are warmer and deeper, submarine melt rates are at their greatest (cf. Seroussi
63 *et al.*, 2011), however, significant complexity around this basic rule is expected. Despite
64 uncertainties, the importance of understanding the magnitude of ice shelf loss, as well as any spatial
65 complexity and variability is significant, because of the potential for ice shelves to collapse with
66 consequent implications for the flow of grounded ice to the oceans, and on overall ice-sheet stability
67 (Dupont and Alley, 2005; 2006; Kulesa *et al.*, 2014). The GzIS is of particular importance because
68 not only is it particularly vulnerable to warming ocean waters, but future predictions suggest
69 warming-induced losses will be most pronounced of all the Antarctic ice shelves, and because of its
70 complexity, there is likely to be considerable spatial variation in the response of the ice shelf to this
71 oceanic warming.

72 In 2013, Jacobs *et al.* collected profiles at sub-ice cavity openings along the GzIS to measure water
73 temperature, salinity and dissolved oxygen content. From satellite-derived measurements of ice flux,
74 modelling and other observations they calculated that through the 2000s, there was marked
75 variability in ice shelf mass balance, with a positive mass balance in 2000 but a negative mass
76 balance in 2007. These observations are invaluable but do not represent absolute and direct
77 measurements of sub-ice melting and to date there have been no direct measurements of such
78 losses on the GzIS. There has, however, recently been an attempt to explore subglacial melting
79 directly on Antarctic ice shelves elsewhere (Khazendar *et al.*, 2016). Khazendar *et al.* (2016) directly
80 quantified submarine melting of the Dotson and Crosson ice shelves in the Amundsen Sea Sector of
81 West Antarctica from observation of repeat Operation IceBridge radio echo-sounding (RES) lines.
82 Amongst their findings, they observed very significant ice loss from beneath – much larger than the
83 rates identified in a recent modelling study by Bernal *et al.* (2017). Clearly then, there is much to
84 be gained from direct observations and measurements, and with that in mind, here we extend the



85 approach of Khazendar et al. (2016) to the GzIS and directly quantify spatially variable ice shelf
86 change.

87

88 3. Methods

89 In order to explore submarine change of the floating GzIS, repeat measurements are required of the
90 ice shelf surface and bottom. Such measurements are available from the Centre for Remote Sensing
91 of Ice Sheets (CRESIS) at the University of Kansas (Gogineni, 2012), and the radio echo sounding
92 (RES) data that they have gathered extensively across both Antarctica and Greenland using an
93 airborne system.

94 Initially, it was the Level 2 (L2) data which we looked to utilise, which provides measurements of ice
95 thickness as well as the elevations of the surface and bottom of the ice. However, we found a
96 number of anomalous points and so elected to go back to the Level 1B data from the Multichannel
97 Coherent Radar Depth Sounder (MCoRDS) – it is these data that are utilised and explored. The
98 benefit of using data from a lower processing level is that it enables picks to be verified or modified
99 first-hand. This RES system has been used to gather data since 1993 using funding from both NASA
100 and the NSF, most recently as part of the Operation IceBridge field campaign (Leuschen and Allen,
101 2014).

102 In November 2010, as part of the Operation Icebridge survey for this year, a flight took place over
103 the GzIS, closely following the linear ice-cliffs of the series of glaciers and ice-streams that drain into
104 the ice-shelf. As part of the Icebridge campaign of 2014, a section of the same survey line was re-
105 flown, again in November of that year (Figure 1). The MCoRDS radar data has an along-track
106 resolution of ~25 m and a depth resolution of ~ 18 m (Khazendar *et al.*, 2016). Using the Level 1B
107 data, each flight was re-examined for anomalous points (often associated with apparent incorrect
108 picking of the bottom reflector, or with inaccurate picking of the reflector) and these were
109 corrected. This was carried out using the Matlab code: ‘image_browser_v1_4’ available via the
110 CRESIS ftp site: <ftp://data.cresis.ku.edu/data/picker/> (CRESIS, 2016), and corrected picks were then
111 compared.

112 Of course, despite these two flights covering effective repeat-tracks, individual sounding locations
113 are not exactly replicated between these four years. In order to maximise the usefulness of these
114 datasets, but also so as to not introduce artefacts, we followed the example of Khazendar *et al.*
115 (2016) and their recent work, by comparing points which are closer than 200 m in the horizontal.
116 Khazendar *et al.* (2016) imposed this limitation in order to reduce the effects of the slope of the ice
117 bottom when exploring change. An identical approach is followed here. The result of this analysis of
118 close overlap between the two survey flights (in 2010 and 2014) delineates the zone over which this
119 study takes place (see Figure 2). This zone covers a large part of the floating Getz ice shelf, and it is
120 this region on which the remainder of this paper is focussed (cf. Figure 1).

121 Once comparable points had been derived, the difference between the elevation of the underside
122 of the floating ice shelf was determined in each year, so as to explore the spatial variability in rates
123 of change at the ice shelf bottom.



124 The use of the MCoRDS radar to determine the ice shelf bottom does introduce some uncertainty,
125 not least because despite every effort to the contrary, flying repeated survey tracks four years apart
126 inevitably results in slightly different flight tracks and thus lightly different regions of the bed are
127 imaged. Figure 3 shows example radargrams from part of the repeated survey line in 2010 and 2014.
128 The region of the domain explored here is shown in green in Figure 2. Examination of Figure 3
129 reveals that despite the limitations indicated, remarkably good repeat-surveying has been achieved.
130 Only very slight differences are visible between these two sampled regions, as a result of slight
131 offsets in the two survey lines Khanzendar *et al.* (2016) go into some detail discussing how they
132 account for errors in the MCoRDS data. They suggest that based on system and environmental
133 parameters, a conservative estimate of vertical measurement uncertainty is ± 25 m, while the
134 uncertainty in measurements of change between two years is ± 35 m. However, they go on to say
135 that when considering annual rates of change in the base elevation, uncertainty is calculated by
136 dividing total change by the time between the two measurements (Khanzendar *et al.*, 2016). As a
137 result, uncertainty estimates when comparing ice bottom changes between 2010 and 2014 is ± 8.75
138 m a^{-1} .

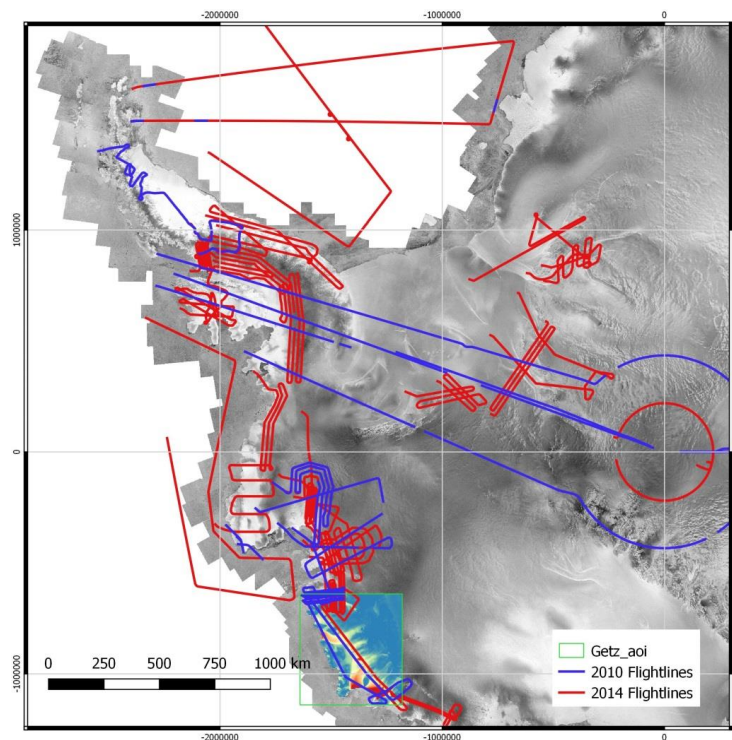


Figure 1: CRESIS flightlines across Antarctica in 2010 (blue) and 2014 (red). The focus of this study is located towards the bottom of the image, and can be identified by the green rectangle and superimposed surface velocities (Rignot *et al.*, 2017; cf. Figure 3). The background image is the MODIS Mosaic of Antarctica (MOA; Scambos *et al.*, 2007; Haran *et al.*, 2013; 2014). All data projected in polar stereographic coordinates.

139

140 In order to confidently identify 'real' changes at the ice-shelf base, it is important to assess if any
141 measured changes may actually be attributable to other erroneous factors (e.g. differences in
142 system parameters from one survey to the next; successfully picking the same basal reflector in both



143 surveys; resolution of the data). In order to do this, we firstly only utilise bed data where the pick-
144 confidence is high (as defined in MCoRDS data description). Furthermore, we also investigated basal
145 elevation change between the four years, focussing on grounded ice areas only. Here, there should
146 be a mean basal height change of zero (as there should be no basal change in grounded ice over this
147 timescale) with scatter around this representing the noise associated with slightly different flight
148 tracks and thus measured positions, as well as differences at the picking stage. We excluded extreme
149 outliers occurring due to gross errors (where differences exceeded 60 m, accounting for just 11.6%
150 of measurement samples), and investigated the relationship between the bed elevations in 2010 and
151 2014 in the remaining data. However, we did not treat all data points as one whole, since this simple
152 solution would assume a constant bias across the whole domain, taking no account of the potential
153 for different biases in different parts of the domain (e.g. a sloping bias). To that end, we explored the
154 differences in bed elevation in the four years in each of the five grounded zones independently.
155 From this investigation we discovered that the domain can be grouped into two regions which show
156 slightly different trends in bed elevation offsets between the two years. In the northern region, a
157 strong, systematic relationship between the bed elevations in 2010 and 2014 exists ($R^2 \sim 1$), with a
158 mean difference of +17.55 m, meaning that the 2014 bed is systematically higher than the 2010 bed.
159 In the southern region, there is also a strong, systematic relationship (R^2 of ~ 1), with a mean
160 difference of +28.73 m, again meaning that the 2014 bed is systematically higher than the 2010 bed
161 here, but by a slightly greater amount. These very strong systematic discrepancies mean we used
162 this information to correct all samples (not just grounded regions) to account for this bias, treating
163 the northern and southern regions differently.

164 Once debiased, we spatially average the along-track height change over samples within a 100m
165 along-track window size. We did this because we observed substantial variability in the bed
166 topography and spatially averaging reduces noise and helps to identify any outliers.

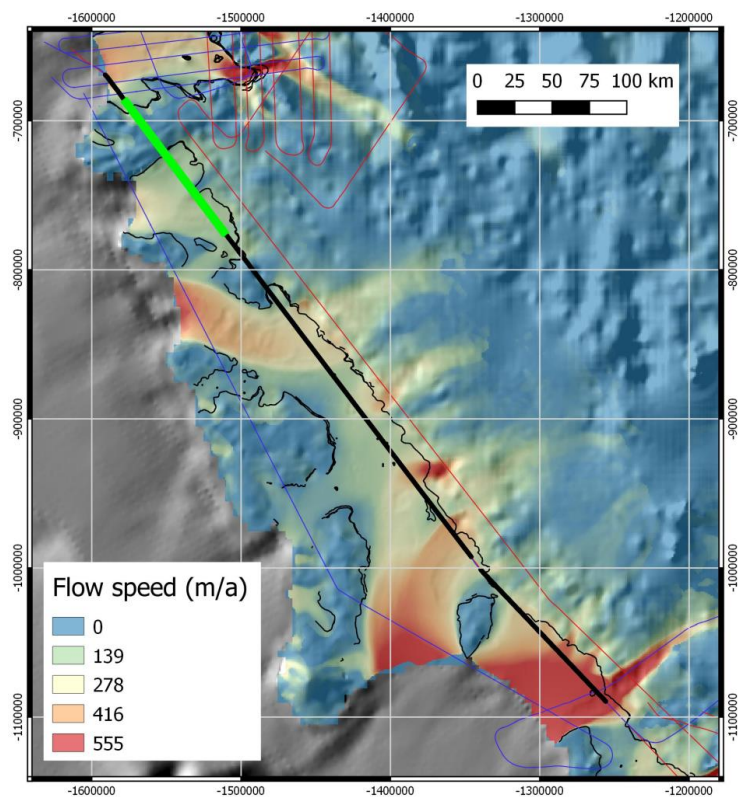


Figure 2: Close-up of area of interest over the Getz Ice Shelf. The thin blue and red lines indicate the IceBridge flightlines from 2010 and 2014 respectively. The thicker black line represents the area of overlap and the data on which this study is focussed. The portion of this black line that is coloured green represents the area covered by the sample radargrams in Figure 3. The thin black line represents the grounding line (Rignot et al., 2011; 2014; 2016). The background (grey-scale) image is a hill-shaded relief map derived from the BEDMAP-2 product (Fretwell et al., 2013). The red/white/blue shaded superimposed background displays surface velocities (Rignot et al., 2017).

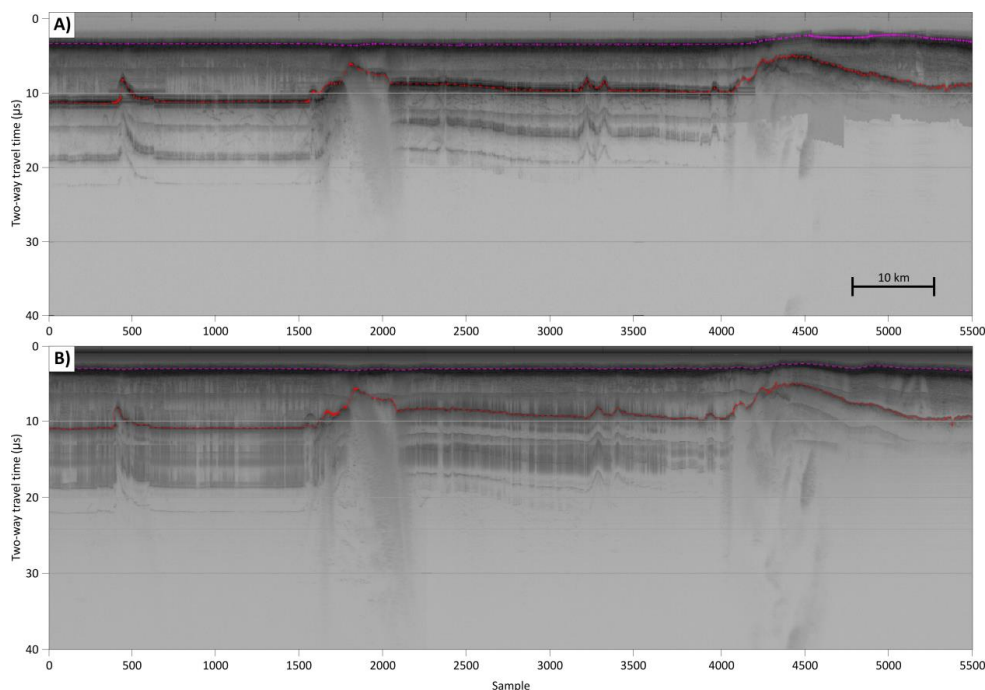


Figure 3: Example radargrams from the Operation Icebridge surveys of November 2010 (A) and November 2014 (B). These two sections represent repeat surveys over the area marked in green in Figure 2. It can be seen here that the two surveys achieved remarkably good repeated sampling locations, although subtle offsets and differences are visible, indicative of slight offsets in the two survey lines. The red dashed lines in both (A) and (B) represent the picked bed while the pink dashed lines represent the picked surface. In both cases, these are the picks provided by CRESIS, with small modifications and corrections made by the author (see main text).

168

169 In addition to investigating changes in the ice shelf bottom, we also investigated changes at the ice
170 surface. This was done using laser altimetry data that were collected on board the survey aircraft at
171 the same time as the RES data (Studinger, 2018). Data were gathered by the IceBridge ATM
172 (airborne topographic mapper) sensor at a spatial resolution of 80 m (sample width) and with a 40 m
173 along-track sample-spacing (Studinger, 2018). However, simply ascertaining changes in surface
174 altitude is not sufficient for understanding and assessing overall change at the surface in Antarctica,
175 because variability is also partly a consequence of changes within the firn layer, which can vary
176 widely (Ligtenberg et al., 2011). As a consequence, in addition to measuring ATM-surface changes,
177 we also explore the role of changes in the firn layer using output from the Regional Atmospheric
178 Climate Model (RACMO2; Ligtenberg et al., 2011). The model was run from January 1979 to
179 December 2015, and over this time period, surface height change was assumed to be zero (in
180 agreement with the model assumptions of steady state over the 35 years of the model run;
181 Ligtenberg et al., 2011). Changes in the firn layer (dH/dt_{firn}) between November 2010 and
182 November 2014 were extracted from the model output, and these were subtracted from observed
183 surface changes from the ATM (dH/dt_{obs}). This final, resultant change in surface elevation
184 (dH/dt_{ice}) is then attributable to a mass loss at the surface due to melt (or thickening due to
185 accumulation). Dynamic processes are also not accounted for, and are discussed later. Any
186 uncertainty in the firn model used to calculate surface change arises from uncertainties in
187 determination of accumulation and snowmelt in the initial spin-up stages of the model (Ligtenberg,
188 personal communication, 2017). Estimates of uncertainty in accumulation are $0.004 \text{ m yr}^{-1} (\% \text{ Acc})^{-1}$,



189 whereas there is an estimated 20% uncertainty in snowmelt quantity. Taken in combination, the
190 greatest uncertainties occur in areas of greater melt (e.g. up to 0.15 m yr^{-1} on the Antarctic
191 Peninsula) while the smallest uncertainties are in cold interior regions ($< 0.0001 \text{ m yr}^{-1}$) (Ligtenberg,
192 personal communication, 2017; cf. Pritchard et al. 2012). Again, for investigating change in the
193 elevation of the ice shelf surface, we follow the example of Khanzendar *et al.* (2016) and only
194 compare points in the different years that fall within the smaller distance of 25 m of each other.
195 Khanzendar *et al.* (2016) state that the uncertainty inherent in these ATM measurements is $< 0.09 \text{ m}$
196 (Krabill et al., 2002), but that where ice is afloat the effects of tides adds additional uncertainty of
197 $0.4\text{-}0.6 \text{ m}$ (Padman et al., 2002). As a result, we take a conservative error uncertainty of 0.7 m over
198 the four-year study period, neglecting all apparent measures of change that are less than this, but
199 annually this equates to 0.175 m/yr .

200 We utilise all of the datasets outlined above to examine the change in ice shelf thickness of the GzIS
201 between, 2010 and 2014 and thus provide the first direct quantification of change at this ice-shelf.

202

203 4. Results and analysis

204 4.1. Changes at the ice-shelf surface

205 Before considering changes occurring at the base of the GzIS, it is important to recognise that total
206 ice thinning can be considered as the sum of changes taking place at both the top and bottom of the
207 ice-shelf. In order to extract thinning that is occurring as a consequence of basal melting, it is
208 necessary to constrain the contributions that come from changes taking place at the surface
209 (Khanzendar et al., 2016). As described in the methodology, we constrained this by considering
210 observed changes from repeat ATM measurements in the domain, and by considering modelled
211 changes in the firn layer. The resultant changes therefore represent changes due to melting or
212 accumulation. In order to constrain the importance of surface changes on overall mass loss, we
213 focussed further attention only on slow moving areas which are grounded. The reason for this is that
214 it is in such regions that it can be assumed that the contribution to overall thinning at the base is
215 zero (because there is no basal melting where the ice is grounded) and the contribution to overall
216 thinning from dynamic processes is minimal. Table 1 summarises the findings of this analysis.

	Min	1st Quart	Median	Mean	3rd Quart	Max
All change	-1.946	-0.712	-0.165	-0.367	0.006	0.814
Rising surf (+ve change)	0.175	0.199	0.231	0.270	0.289	0.814
Lowering surf (-ve change)	-1.946	-1.085	-0.733	-0.775	-0.452	-0.176

Table 1: Summary statistics of the magnitude of annual change (m a^{-1}) at the ice surface elevation between 2010 and 2014 in areas of slow-moving grounded ice (cf. Figure 4). Surface elevation change ($\text{dH}/\text{dt}_{\text{ice}}$; m a^{-1}) is derived from measurements of repeated ATM observations ($\text{dH}/\text{dt}_{\text{obs}}$) and changes in the firn layer ($\text{dH}/\text{dt}_{\text{firn}}$) from the RACMO2 model (Ligtenberg et al., 2011). Data are subdivided into regions where the ice surface is rising (positive change) or lowering (negative change).

217

218 In this region, where changes are greater than uncertainties, 87.35% of point locations (746 of 854)
219 experiences surface lowering, with just 12.65% of locations (108 of 854) experiencing thickening. In
220 the small number of areas where thickening has occurred, the mean rate is nearly three times less
221 than where thinning has occurred. However, overall, these values are small, particularly when
222 compared with changes at the bed (cf. Table 3, but discussed later). Nevertheless, there is variability



223 in rates of accumulation (or otherwise) and we suggest that this variation can be explained by
224 altitudinal effects. The mean altitude where thinning takes place is 308.9 m whereas where
225 thickening dominates it is 504.2 m. Khazendar et al. (2016), in their work on the Dotson and Crosson
226 Ice Shelves, also found such altitudinal-controlled variability, suggesting that the relative role and
227 importance of air temperature, accumulation rate, as well as other factors that are influenced by
228 surface elevation change, might vary, and thus explain why mass loss or gain at the ice surface might
229 be experienced across the domain. Where they identified surface lowering (our dominant signal),
230 this was in the range of $0.4\text{--}0.7\text{ m a}^{-1}$, and the values we record here are in very close agreement
231 with these.

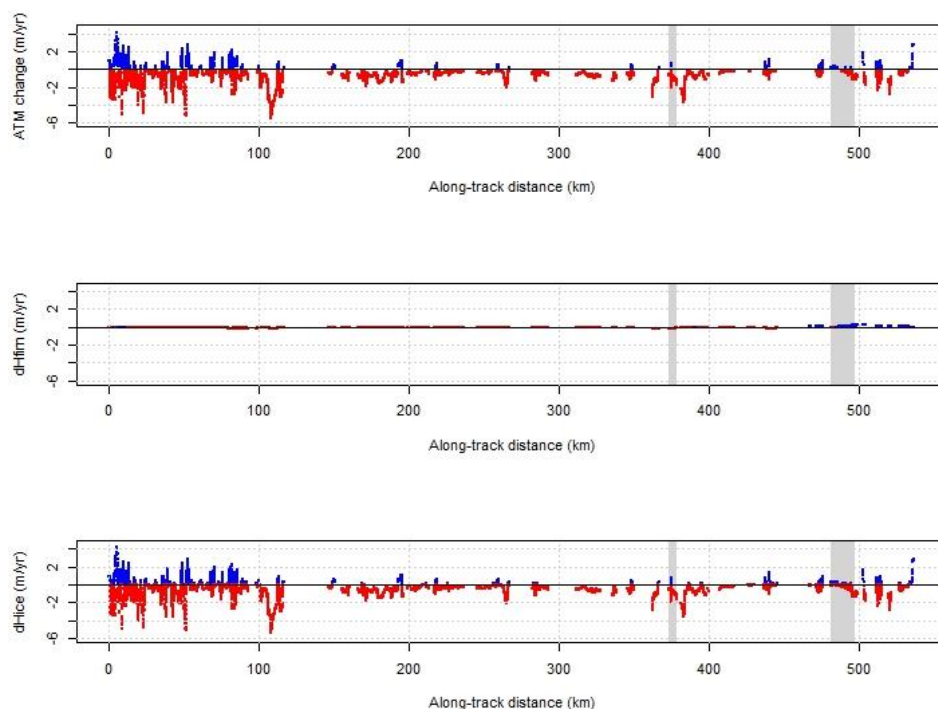


Figure 4: Annual change in ice-surface elevation (m a^{-1}) between 2010 and 2014 along the entire survey domain. The upper panel shows rates of surface change as derived from the repeat ATM measurements. The middle panel shows rates of surface elevation change based on changes in the firm layer, as derived from the RACMO2 firm densification model (FDM). The lower panel shows the residual change in surface elevation after considering firm densification processes. These changes are attributable to a mass loss due to melt. In all panels, blue dots indicate a positive elevation change meaning a rising ice surface and thus a thickening, while red dots indicate a negative elevation change meaning a lowering ice surface and thus a thinning. The black horizontal line represents no change. Grey shaded areas indicate where ice is slow-moving and grounded and thus minimal change would be expected. With reference to Figure 2, zero along-track distance in the above panels is associated with the southern-most points in the transect.

232

233 **4.2. Changes at the ice-shelf bottom**

234 We initially explored the annual rate of basal change along the whole survey-line from 2010 and
235 2014, but then subsequently subdivided the domain into those regions which we classify as being
236 within a floating ice-shelf, and others classified as being grounded (Figure 5).

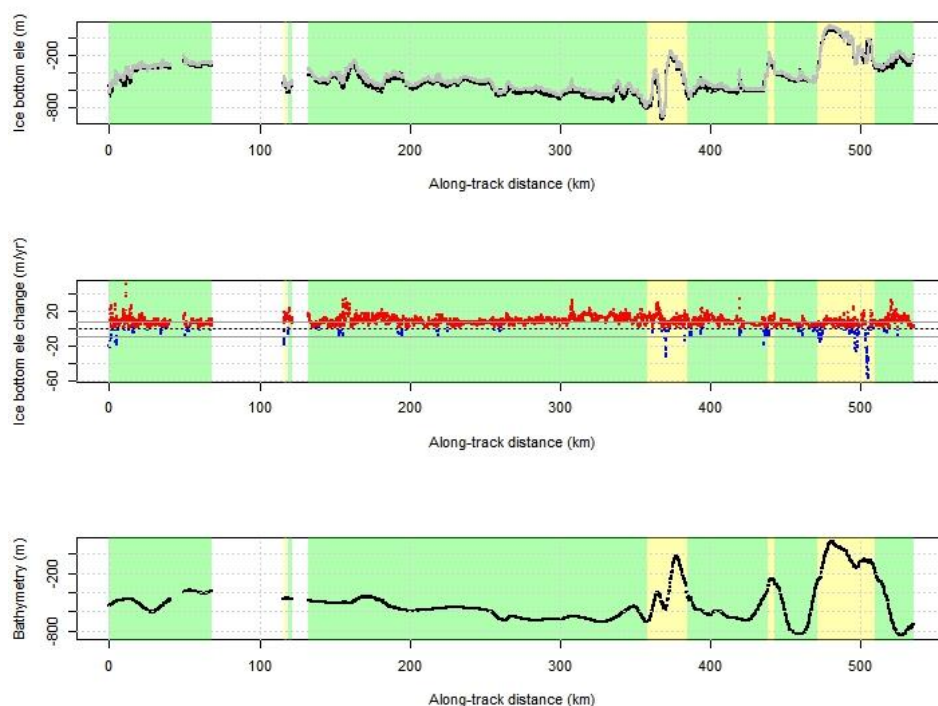


Figure 5: Annual change in ice-base elevation between 2010 and 2014 along the entire survey domain, with the 2014 bed elevations debiased according to the methodology described. The upper panel shows how the ice-bottom has changed between 2010 and 2014. The black line represents the bottom in 2010 and the grey line in 2014 (debiased). Data shown here are raw bed elevations. In the second panel, rates of bottom elevation change (m a^{-1}) are shown, with elevation change spatially averaged over 100m-long windows. In the middle panel, red dots indicate a positive elevation change meaning a rising ice bottom and thus ice-shelf thinning. Blue dots indicate a negative elevation change meaning a lowering ice bottom and thus ice-shelf thickening. The grey horizontal lines represent the bounds of uncertainty – values must indicate changes of magnitudes greater than these limits to be indicative of real change (see text). The lower panel indicates the bathymetry of the sea-bed at each point derived from the International Bathymetric Chart of the Southern Ocean (BCSO v1.0; Amdt et al., 2013). Areas with a green background are areas where floating ice-shelves are present. Areas with a yellow background are where ice is grounded (cf. Figure 2 for location of survey domain). Note the significant data-gap between ~75-120 km along track. Here, bed picks are of lower confidence in one or both of the two surveys, and so data here is not included to avoid introducing erroneous measurements of change.

237

238 In Figure 5, a positive change reflects a rising of the ice-base and thus thinning and mass loss.
239 Conversely, a negative change reflects a lowering of the ice-base and thus a thickening or mass gain.
240 Perhaps the most important panel in Figure 5 is the middle panel because this indicates the overall
241 amount of change at the ice-shelf bottom. Red symbols in this panel (in Figure 5) represent a rising
242 ice-bottom, and where this change reaches beyond the margins of error (grey horizontal lines in
243 these panels) then we consider this rising ice-bottom to be real. It can also be seen that in some
244 locations (where blue symbols are visible) the ice-base has lowered. These locations are more
245 sparsely distributed, but nevertheless it is important to consider where these areas of apparent ice-
246 bottom lowering (and indeed rising) are located.

247 Of all the spatially-averaged sample points along this line (5357 in total), 71.46% are classified as
248 being within floating ice shelves, while 7.62% are associated with grounded ice (the remaining
249 20.93% are generally associated with no data (due to the exclusion of low-confidence picks). Where



250 picks are high quality however, 90.37% (3828) are classified as being within floating ice shelves,
 251 while 9.63% (408) are associated with grounded ice.

252 Considering floating and grounded ice together, 4350 (81.20%) show a rising of the ice-base (and
 253 thus thinning) with just 299 (5.58%) indicating a lowering of the ice base (and thus thickening).
 254 However, many of these points are within the error margins of ± 8.75 m discussed previously – only
 255 48.04% of all points show any sort of change larger than the margins of uncertainty. Of these points
 256 alone, 82.75% are within floating ice shelves and just 10.86% are within grounded ice. Table 2
 257 summarises the changes that have taken place where the observed change is greater than the
 258 uncertainty.

259

	No. of points	% of total
Total number of samples	2035	100 %
Ice shelf – rising base (thinning)	1668	81.97 %
Ice shelf – lowering base (thickening)	16	0.79 %
Grounded ice – rising base (thinning)	195	9.58 %
Grounded ice – lowering base (thickening)	26	1.28 %

Table 2: Summary of changes at the ice-base where spatially-averaged changes are greater than the suggested error of ± 8.75 m. The table shows the number of points and also the relative dominance of each class as a proportion of the total number of sample points where change is larger than uncertainty. The data is split into areas of floating ice-shelves and grounded ice, as well as being further subdivided into areas where the apparent change is positive (i.e. meaning a rising ice base and thus thinning) or negative (i.e. a lowering ice base and thus thickening).

260

261 Table 2 shows that it is on the floating ice-shelves where change at the base is of greatest
 262 significance, and apparent rising of the ice base is the dominant signal (81.97% of all points where
 263 change is greater than errors). On the ice-shelf alone, positive change (i.e. thinning of the base) is
 264 apparent in 99.05% of all ice-shelf measurements that are greater than errors. In just 0.95% of cases
 265 ice shelf thickening is apparent. Table 3 shows the magnitude of the changes taking place in these
 266 floating-ice regions. It is important to note that the changes at the base here are two orders of
 267 magnitude greater than those at the surface (cf. Table 1) rendering the changes and uncertainties at
 268 the surface almost irrelevant by comparison. Clearly then, while there is some spatial variability,
 269 significant thinning of floating ice is the dominant signal in the domain.

	Min	1st Quart	Median	Mean	3rd Quart	Max
Thinning (+ve change)	8.75	9.99	11.66	12.85	14.58	52.24
Thickening (-ve change)	-21.61	-17.92	-14.13	-14.23	-9.31	-8.90

Table 3: Summary statistics of the magnitude of change ($m a^{-1}$) at the ice base in floating ice-shelves where change is greater than the measure of uncertainty (± 8.75 m). Data are subdivided into regions where the ice-shelf base is thinning or rising (positive change) and where it is thickening or lowering (negative change). Note that although the magnitude of mean thickening is greater than the thinning, thickening takes place over a much smaller number of measurement locations.

270

271 With respect to the thickening regions of floating ice shelf (where greater than errors), although
 272 these regions are relatively sparse, close analysis of bathymetry data from the International
 273 Bathymetric Chart of the Southern Ocean (IBCSO v1.0; Arndt et al., 2013; cf. bottom panel of Figure
 274 5) suggests that they may arguably be most prominent where the bed topography is most variable
 275 (e.g. at ~ 0 -75 m along-track and ~ 420 -430 m along-track). In such regions, slope-changes are larger,
 276 perhaps reflecting locations where floating ice abuts grounded ice, and thus inaccuracies in



277 delineating the boundary between these two are apparent. We consider this further in the
278 discussions.

279 Figure 6 shows the distribution of the magnitude of ice-base thinning and thickening (where
280 measurements are greater than uncertainty), while Figure 7 shows where the greatest amount of
281 ice-bottom melting has taken place. Figure 6 clearly demonstrates that the greatest signal is one of
282 ice-base thinning in floating ice, and that overall, an annual ice-base loss of $\sim 10\text{-}20\text{ m a}^{-1}$ is most
283 common, with a few areas experiencing losses of 2-3 times this.

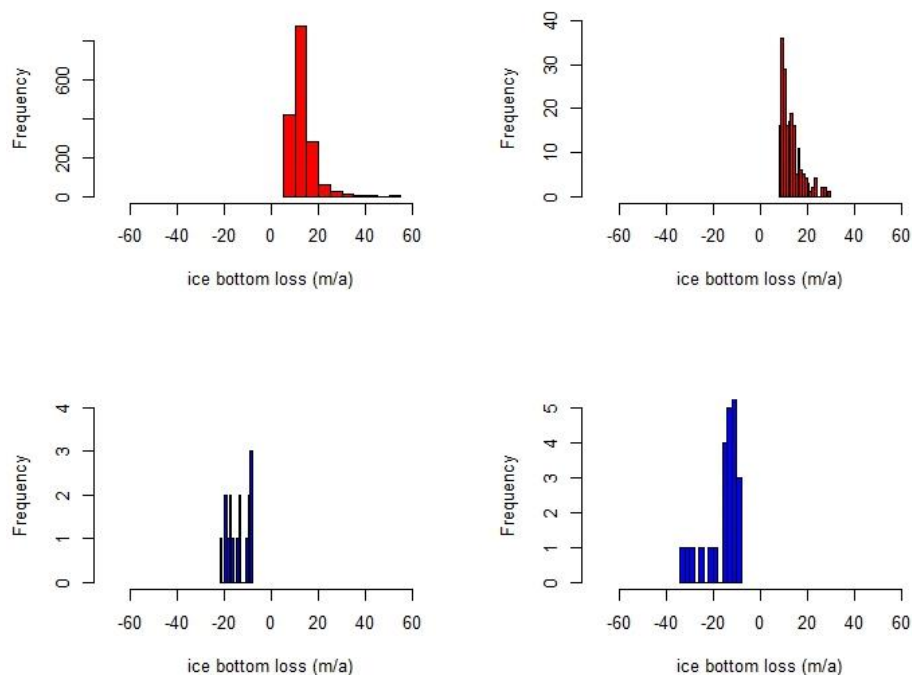


Figure 6: Histograms showing the amount of ice-bottom change experienced where the ice is floating (left-hand panels) and where it is grounded (right-hand panels), with thinning displayed in red in the top two panels, and thickening displayed in blue in the bottom two panels (only where greater than uncertainties). Where ice bottom loss is positive, this represents thinning between 2010 and 2014. Where ice bottom loss is negative, this represents thickening between 2010 and 2014. Note the markedly different y-axis scales. It is very clear that thinning dominates, and that this thinning is much more pronounced and widespread where the ice is afloat.

284

285 Figure 7 shows the locations where these losses are at their greatest and it can be seen that in
286 general there is a tendency towards greater ice loss in locations where the ice is fastest flowing (left-
287 hand panel). In slower-flowing regions, changes are perhaps smaller. This relationship suggests there
288 may be a dynamic thinning component, in which some ice loss occurs due to dynamic processes. This
289 is dealt with further in the Discussions.

290

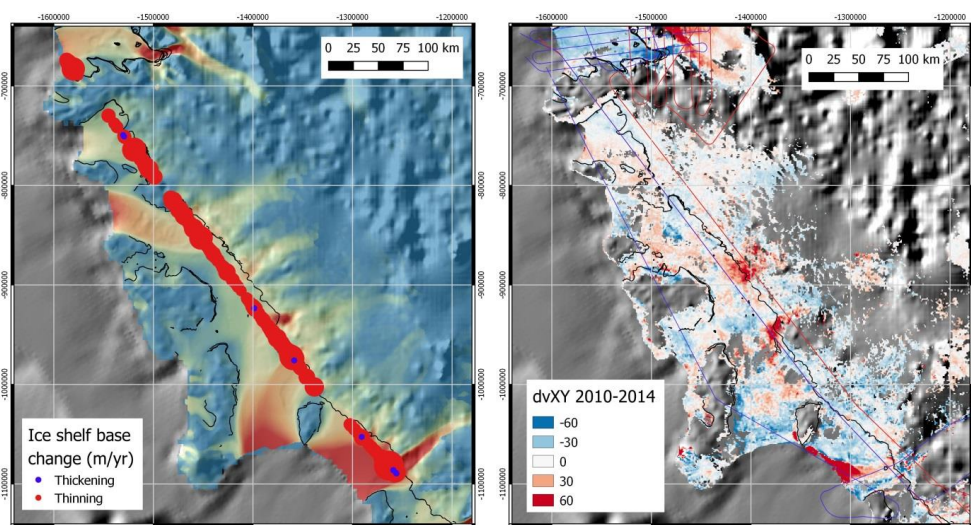


Figure 7: Left-hand panel shows ice shelf thinning (red circles) and thickening (blue circles) where change is greater than the margins of uncertainty, and only where ice is floating. Ice loss (thinning) is greatest where ice velocities are higher. The black line represents the grounding line (Rignot et al., 2011; 2014; 2016). The background (grey-scale) image shows bathymetry data from the International Bathymetric Chart of the Southern Ocean (IBCSO v1.0; Arndt et al., 2013). The red/white/blue shaded superimposed background displays surface velocities with red regions indicating fast flow and blue areas indicating slow flow. (Rignot et al., 2017). In the right-hand panel, changes in surface velocity are displayed, derived from the MEASURES Annual Antarctic Ice Velocity Maps 2005-2016 (Mouginot et al. 2017). Here we display the difference between two datasets, one of velocities from 2010-2011 and another from 2014-2015.

291

292 Where changes are apparently occurring at the base of grounded ice, it is important to keep in mind
 293 that all change in grounded regions accounts for a relatively small proportion of those sampled
 294 locations (10.86% of all data; Figure 6; cf. Table 4). Nevertheless, it is important to note that the
 295 apparent changes here are not insignificant.

	Min	1st Quart	Median	Mean	3rd Quart	Max
Thinning (+ve change)	8.75	9.92	12.10	13.14	14.69	29.43
Thickening (-ve change)	-33.09	-15.09	-12.89	-15.30	-10.84	-8.88

Table 4: Summary statistics of the magnitude of change (m a^{-1}) at the ice base in regions of grounded ice where change is greater than the measure of uncertainty ($\pm 8.75 \text{ m}$). Data are subdivided into regions where the ice-shelf base is thinning or rising (positive change) and where it is thickening or lowering (negative change).

296

297 Such change under grounded ice is somewhat surprising, since, at the ice base, it would be expected
 298 that there would be no such change – at this location, over the timescale being explored, the ice
 299 base should effectively be static. However, we propose that this apparent change is in fact not
 300 indicative of real change, but is in part a function of an uneven (or rough) subglacial topography in
 301 which correct identification of the bed reflector is not straightforward and is indeed prone to errors.
 302 Under scenarios where a complex bed topography dominates, both along-track and off-track, it is
 303 highly likely that the bed is incorrectly picked between consecutive years (cf. Lapazaran et al., 2016).
 304 Indeed, we encountered this in our own investigations and adapted our methodology to go some
 305 way towards incorporating this (see Methods). It is also highly likely that precisely the same track is
 306 not taken between surveys, further introducing errors. Finally, a relatively large component in the
 307 error is likely a result of uncertainties in the aircraft flying height during data collection. In some



308 locations however, such discrepancies may be due to real changes, which will be discussed further in
309 the discussions.

310

311 5. Discussions and Conclusions

312 For a long time, the main cause of mass loss from the Antarctic Ice Sheet was considered to be
313 iceberg calving (Depoorter et al., 2013). More recently, melting of floating ice due to a warming
314 ocean has been shown to be significant, particularly close to the grounding line and near the calving
315 front (Jenkins and Doake, 1991; Rignot and Jacobs, 2002; Joughin and Padman 2003). However,
316 direct measurements of basal ice shelf change in Antarctica are sparse. While Khazendar et al. (2016)
317 were the first to show direct evidence of ice-shelf thinning from repeat RES measurements, here we
318 have presented the first direct measurements of ice shelf change on the large GzIS using repeated
319 airborne RES surveys. Comparison of the recent modelling output from Bernales *et al.* (2017) with
320 the measurements of Khazendar *et al.* (2016) shows that the models underestimate the amount of
321 basal melting, and given that it is the Amundsen Sea (including the GzIS) where greatest changes are
322 forecast to happen in the decades to come (Naughten *et al.*, 2018), assessing whether such
323 discrepancies exist here is of importance. As a result, we have investigated the magnitude and
324 nature of change at both the surface and the base. When exploring surface changes, we found that
325 these are small compared to those observed at the bed, by up to two orders of magnitude, and thus
326 in this study over the GzIS, surface lowering can, to all intents and purposes, be ignored. The
327 changes taking place at the ice base are far greater and far more significant, and so it is therefore
328 this location where we focus the remains of this discussion.

329 In terms of basal changes, floating ice dominates the domain, and it is here that changes are of
330 greatest magnitude, of greatest interest and also of greatest significance. Where ice is floating and
331 where changes are significant, thinning was observed in nearly 82% of locations, at a mean rate of
332 nearly 13 m a^{-1} , but up to a maximum of $\sim 52 \text{ m a}^{-1}$. These values are (on average) slightly smaller
333 than, but nevertheless comparable with, the $40\text{--}70 \text{ m a}^{-1}$ recorded by Khazendar et al. (2016) the
334 Dotson and Crosson ice shelves. Furthermore, the rates of change that are identified here are
335 substantially greater than those reported by Bernales *et al.* (2017) in their extensive modelling study
336 of basal changes around Antarctica. Their model suggests melting rates of $2.5 / 4.3 \text{ m w.e. a}^{-1}$
337 (equilibrium/non-steady state values) which are several times lower than our measurements. The
338 identification of substantially higher rates of loss is of great concern because it means it is losing
339 mass more quickly than previously thought, with significance for the rates at which ice is transmitted
340 through the glaciers which drain into the GzIS. While thinning occurred over most of the domain, the
341 biggest rates of thinning occurred where ice flowed more quickly (cf. Figure 7) perhaps also
342 indicating a role for dynamic processes in the observed thinning. Dynamic thinning is a loss of ice as
343 a result of accelerated flow (Pritchard et al., 2009). While not a true measure of dynamic thinning
344 itself, increasing ice flow may lead to the dynamic thinning of a glacier (Bevan et al., 2015), and so by
345 assessing changes in ice velocity (as well as velocity itself), the relative likely importance of the
346 dynamic thinning process can be ascertained. The observations we make are thus further reinforced
347 by Chuter et al. (2017) who identified variable rates of grounding line velocity increases (2007-2014),
348 but particularly a coincidence between the largest grounding-line velocity increases and regions of
349 greatest ice-shelf thinning (Chuter et al., 2017; their Figure 4). We therefore suggest that some of



350 the observed thickness change on the GzIS may be attributable to dynamic processes rather than
351 direct mass loss at the bottom (or indeed the surface) of the ice-shelf.

352 Changes greater than uncertainty over grounded ice accounts for approximately 10.86% of the
353 survey domain. Where ice is grounded, the complex subglacial topography makes it difficult to
354 accurately pick the terrain, and as a result, there is some uncertainty surrounding the basal
355 variability. However, in ~13% of locations we observe apparent shelf thinning over grounded ice, and
356 it is possible that some of this apparent thinning may be attributable to ice-shelf ungrounding
357 between the two surveys. We have no evidence of this having occurred but Schaffer *et al.* (2016)
358 propose the existence of continuous troughs that link the open ocean to the grounding line, and
359 propose that high basal melt rates here support the existence of a routeway along which warm
360 ocean waters may access the ice base. This proposal, though untested would perhaps allow melting
361 of grounded ice at the grounding line, and thus a degree of ungrounding, as we propose.

362 Our work highlights firstly, and crucially, that thinning is both significant and widespread across
363 much of the GzIS. Secondly, it highlights that despite this, there is significant variability in ice-shelf
364 bottom change, reinforcing the point made in the *Introduction* that ice shelf complexity has an
365 important role to play in controlling the way and rate by which an ice-shelf responds to oceanic
366 warming. Finally, and perhaps most importantly, our work identifies substantially greater rates of
367 thinning than those recently reported from forecasting modelling investigations (Bernales *et al.*,
368 2017). While we accept that our work represents investigations along a single transect, the
369 difference between predictions from models and direct historical measurements (c.f. Khazendar *et al.*,
370 2016) is clearly of concern. This suggests that models may be underestimating changes going on
371 in at least some parts of some ice shelves, and thus more and continuous direct measurements of
372 change are required. This is firstly to help better constrain models, and secondly to better constrain
373 the changes actually occurring in ice shelves.

374 Depoorter *et al.* (2013) state that the significance of basal processes in overall ice shelf mass balance
375 is highly variable, accounting for 10-90% of overall loss, depending on the specific ice shelf in
376 question. Here, we have shown that basal melting is a significant contributor to mass loss of the
377 GzIS, but also that the relative contribution of basal melting is highly variable across the ice shelf.
378 This variability within a single ice shelf, coupled with the apparent variability between ice shelves
379 (Depoorter *et al.*, 2013) is significant. In the GzIS, the variability can perhaps be attributed to the
380 combination of complex sub-ice topography and numerous contributory ice streams and outlet
381 glaciers that result in intricate sub-ice water circulation in cavity systems. Although the accuracy of
382 this interpretation requires further investigation, the importance of these processes in overall ice
383 shelf mass balance is undeniable. It is therefore of paramount importance that quantifying basal
384 mass loss from Antarctic ice shelves is carried out, because of its role and importance for predicting
385 the likely vulnerability of ice shelves to future subglacial warming and melting.

386

387 6. Acknowledgements

388 We acknowledge the use of data and/or data products from CReSIS generated with support from the
389 University of Kansas, NSF grant ANT-0424589, and NASA Operation IceBridge grant NNX16AH54G.



390 We also acknowledge Stefan Ligtenberg and Jan Lenaerts for the provision of (and assistance with)
391 RACMO2 data.

392

393 7. References

394 Arndt, J.E., Schenke, H.W., Jakobsson, M., Nitsche, F., Buys, G., Goleby, B., Rebesco, M., Bohoyo, F.,
395 Hong, J.K., Black, J., Greku, R., Udintsev, G., Barrios, F., Reynoso-Peralta, W., Morishita, T., Wigley,
396 R. The International Bathymetric Chart of the Southern Ocean (IBCSO) Version 1.0 - A new
397 bathymetric compilation covering circum-Antarctic waters, *Geophysical Research Letters*, **40**, p.
398 3111-3117, doi: 10.1002/grl.50413, 2013.

399 Berger, S., Drews, R., Helm, V., Sun, S. and Pattyn, F. Detecting high spatial variability of ice shelf
400 basal mass balance, Roi Baudouin Ice Shelf, Antarctica, *The Cryosphere*, **11**, 2675-2690.
401 <https://doi.org/10.5194/tc-11-2675-2017>, 2017.

402 Bernales, J., Rogozhina, I. and Thomas, M. Melting and freezing under Antarctic ice shelves from a
403 combination of ice-sheet modelling and observations. *Journal of Glaciology*, **63**(240), 731–744,
404 doi: 10.1017/jog.2017.42. Bevan, S.L., A. Luckman, S.A. Khan and T. Murray. 2015. Seasonal
405 dynamic thinning at Helheim Glacier, *Earth and Planetary Science Letters*, **415**, 47-53. DOI:
406 10.1016/j.epsl.2015.01.031, 2017.

407 Bevan, S.L., Luckman, A., Khan, S.A. and Murray, T. Seasonal dynamic thinning at Helheim Glacier.
408 *Earth and Planetary Science Letters*, **415**, 47-53, 2015.

409 Bindshadler, R., Choi, H., Wichlacz, A., Bingham, R., Bohlander, J., Brunt, K., Corr, H., Drews, R.,
410 Fricker, H., Hall, M., Hindmarsh, R., Kohler, J., Padman, L., Rack, W., Rotschky, G., Urbini, S.,
411 Vornberger, P., and Young, N.: Getting around Antarctica: new high-resolution mappings of the
412 grounded and freely-floating boundaries of the Antarctic ice sheet created for the International
413 Polar Year, *The Cryosphere*, **5**, 569-588, <https://doi.org/10.5194/tc-5-569-2011>, 2011.

414 CReSIS. Radar Depth Sounder (MCoRDS) Data, Lawrence, Kansas, USA. Digital Media.
415 <http://data.cresis.ku.edu/>, 2016.

416 Chuter, S.J., Martín-Español, A., Wouters, B. and Bamber, J.L. Mass balance reassessment of glaciers
417 draining into the Abbot and Getz Ice Shelves of West Antarctica, *Geophysical Research Letters*,
418 **44**, doi:10.1002/2017GL073087, 2017.

419 Depoorter, M.A., Bamber, J.L., Griggs, J.A., Lenaerts, J.T.M., Ligtenberg, S.R.M., van den Broeke, M.R.
420 and Moholdt, G. Calving fluxes and basal melt rates of Antarctic ice shelves, *Nature*, **502**, 89–92,
421 2013.

422 De Rydt, J., Gudmundsson, G.H. Rott, H. and Bamber, J.L. Modeling the instantaneous response of
423 glaciers after the collapse of the Larsen B Ice Shelf, *Geophys. Res. Lett.*, **42**, 2015.

424 Dupont, T.K. and Alley, R.B. Assessment of the importance of ice-shelf buttressing to ice-sheet flow.
425 *Geophysical Research Letters*, **32**(4), 2005.



- 426 Dupont, T.K. and Alley, R.B. Role of small ice shelves in sea-level rise, *Geophysical Research Letters*,
427 **33**(9), 2006.
- 428 Fretwell, P., Pritchard, H. D., Vaughan, D. G., Bamber, J. L., Barrand, N. E., Bell, R., Bianchi, C.,
429 Bingham, R. G., Blankenship, D. D., Casassa, G., Catania, G., Callens, D., Conway, H., Cook, A. J.,
430 Corr, H. F. J., Damaske, D., Damm, V., Ferraccioli, F., Forsberg, R., Fujita, S., Gim, Y., Gogineni, P.,
431 Griggs, J. A., Hindmarsh, R. C. A., Holmlund, P., Holt, J. W., Jacobel, R. W., Jenkins, A., Jokat, W.,
432 Jordan, T., King, E. C., Kohler, J., Krabill, W., Riger-Kusk, M., Langley, K. A., Leitchenkov, G.,
433 Leuschen, C., Luyendyk, B. P., Matsuoka, K., Mouginot, J., Nitsche, F. O., Nogi, Y., Nost, O. A.,
434 Popov, S. V., Rignot, E., Rippon, D. M., Rivera, A., Roberts, J., Ross, N., Siegert, M. J., Smith, A. M.,
435 Steinhage, D., Studinger, M., Sun, B., Tinto, B. K., Welch, B. C., Wilson, D., Young, D. A., Xiangbin,
436 C., and Zirizzotti, A.: Bedmap2: improved ice bed, surface and thickness datasets for Antarctica,
437 *The Cryosphere*, **7**, 375–393, <https://doi.org/10.5194/tc-7-375-2013>, 2013. Gogineni, P. 2012.
438 CReSIS MCoRDS Level 2 Data, Lawrence, Kansas, USA. Digital Media. <http://data.cresis.ku.edu/>.
- 439 Haran, T., Bohlander, J., Scambos, T., Painter, T. and Fahnestock, M. MODIS Mosaic of Antarctica
440 2003-2004 (MOA2004) Image Map. [indicate subset used]. Boulder, Colorado USA: National Snow
441 and Ice Data Center, <http://dx.doi.org/10.7265/N5ZK5DM5>, 2005, updated 2013.
- 442 Haran, T., Bohlander, J., Scambos, T., Painter, T. and Fahnestock, M. MODIS Mosaic of Antarctica
443 2008-2009 (MOA2009) Image Map. [indicate subset used]. Boulder, Colorado USA: National Snow
444 and Ice Data Center, <http://dx.doi.org/10.7265/N5KP8037>, 2014.
- 445 Holt, T. O., Glasser, N. F., Quincey, D. J., and Siegfried, M. R. Speedup and fracturing of George VI Ice
446 Shelf, Antarctic Peninsula, *The Cryosphere*, **7**, 797–816, <https://doi.org/10.5194/tc-7-797-2013>,
447 2013.
- 448 Horne, E.P. Ice-induced vertical circulation in an Arctic fjord. *J. Geophys. Res.* **90**, 1078–1086, 1985.
- 449 Jacobs, S. S., and Giulivi, C. F. Large multidecadal salinity trends near the Pacific-Antarctic continental
450 margin, *J. Clim.*, **23**, 4508–4524, doi:10.1175/2010JCLI3284.1, 2010.
- 451 Jacobs, S., Jenkins, A., Hellmer, H., Giulivi, C., Nitsche, F., Huber, B. and Guerrero, R. The Amundsen
452 Sea and the Antarctic ice sheet, *Oceanography*, **25**(3), 154–163, 2012.
- 453 Jacobs, S., Giulivi, C., Dutrieux, P., Rignot, E., Nitsche, F. and Mouginot, J. Getz Ice Shelf melting
454 response to changes in ocean forcing, *Journal of Geophysical Research: Oceans*, **118**, 4152–4168,
455 doi:10.1002/jgrc.20298, 2013.
- 456 Jenkins, A. and Doake, C.S.M. Ice-ocean interaction on Ronne Ice Shelf, Antarctica, *J. Geophys. Res.*
457 **96**, 791–813, 1991.
- 458 Joughin, I. and Padman, L. Melting and freezing beneath Filchner-Ronne Ice Shelf, Antarctica.
459 *Geophys. Res. Lett.* **30**, 1477, 2003.
- 460 Khazendar, A., Rignot, E., Schroeder, D. M., Seroussi, H., Schodlok, M. P., Scheuchl, B., Mouginot, J.,
461 Sutterley, T. C., and Velicogna, I.: Rapid submarine ice melting in the grounding zones of ice
462 shelves in West Antarctica, *Nat. Commun.*, **7**, 13243, <https://doi.org/10.1038/ncomms13243>,
463 2016.



- 464 Krabill, W., Abdalati, W., Frederick, E., Manizade, S., Martin, C., Sonntag, J., Swift, R., Thomas, R. and
465 Yungel, J. Aircraft laser altimetry measurement of elevation changes of the Greenland ice sheet:
466 Technique and accuracy assessment. *J. Geodyn.*, **34**, 357-376, 2002.
- 467 Kulesa, B., Jansen, D., Luckman, A. J., King, E., and Sammonds, P. R. Marine ice regulates the future
468 stability of a large Antarctic ice shelf, *Nat. Commun.*, **5**, 3707, doi.org/10.1038/ncomms4707,
469 2014.
- 470 Lapazaran, J.J., Otero, J., Martín-Espanõl, A. and Navarro, F.J. On the errors involved in ice-thickness
471 estimates I: ground-penetrating radar measurement errors. *Journal of Glaciology*, **62**(236), 1008-
472 1020, 2016.
- 473 Leuschen, C. and Allen, C. IceBridge MCoRDS L2 Ice Thickness, Boulder, Colorado, USA, National
474 Snow and Ice Data Centre (2010, updated 2014), 2014.
- 475 Ligtenberg, S. R. M., Helsen, M. M., and van den Broeke, M. R. An improved semi-empirical model
476 for the densification of Antarctic firn, *The Cryosphere*, **5**, 809–819, [https://doi.org/10.5194/tc-5-](https://doi.org/10.5194/tc-5-809-2011)
477 809-2011, 2011.
- 478 Motyka, R., Hunter, L., Echelmeyer, K. and Connor, C. Submarine melting at the terminus of a
479 temperate tidewater glacier, Leconte Glacier, Alaska, USA. *Ann. Glaciol.* **36**, 57–65, 2003.
- 480 Mouginot, J., Scheuchl, B. and Rignot, E. MEaSURES Annual Antarctic Ice Velocity Maps 2005-2017,
481 Version 1. [2010-2011]. Boulder, Colorado USA. NASA National Snow and Ice Data Center
482 Distributed Active Archive Center. doi: <https://doi.org/10.5067/9T4EPQXTJYW9>. [12th October
483 2017], 2017, updated 2017.
- 484 Naughten, K.A., Meissner, K.J., Galton-Fenzi, B.K., England, M.H., Timmermann, R. and Hellmer, H.H.
485 Future Projections of Antarctic Ice Shelf Melting Based on CMIP5 Scenarios, *Journal of Climate*,
486 <https://doi.org/10.1175/JCLI-D-17-0854.1>, 2018.
- 487 Padman, L., Fricker, H. A., Coleman, R., Howard, S., and Erofeeva, L. A new tide model for the
488 Antarctic ice shelves and seas, *Ann. Glaciol.*, **34**, 247–254, 2002.
- 489 Pritchard, H. D., Arthern, R. J., Vaughan, D. G., and Edwards, L. A.: Extensive dynamic thinning on the
490 margins of the Greenland and Antarctic ice sheets, *Nature*, **461**, 971–975,
491 doi.org/10.1038/nature08471, 2009.
- 492 Pritchard, H. D., Ligtenberg, S. R. M., Fricker, H. A., Vaughan, D. G., van den Broeke, M. R., and
493 Padman, L. Antarctic ice-sheet loss driven by basal melting of ice shelves, *Nature*, **484**, 502–505,
494 doi.org/10.1038/nature10968, 2012.
- 495 Rignot, E. and Jacobs, S.S. Rapid bottom melting widespread near Antarctic ice sheet grounding lines.
496 *Science*, **296**, 2020-2023, 2002.
- 497 Rignot, E., Mouginot, J., and Scheuchl, B. Ice Flow of the Antarctic Ice Sheet, *Science*. **333**. 14271430.
498 <http://dx.doi.org/10.1126/science.1208336>, 2011.



- 499 Rignot, E., Mouginot, J., and Scheuchl, B. Antarctic grounding line mapping from differential satellite
500 radar interferometry, *Geophys. Res. Lett.*, **38**, L10504, doi.org/10.1029/2011GL047109, 2011.
- 501 Rignot, E., Jacobs, S., Mouginot, J., and Scheuchl, B.: Iceshelf melting around Antarctica, *Science*, **341**,
502 266–270, doi.org/10.1126/science.1235798, 2013.
- 503 Rignot, E., Mouginot, J., Morlighem, M., Seroussi, H., and Scheuchl, B. Widespread, rapid grounding
504 line retreat of Pine Island, Thwaites, Smith, and Kohler glaciers, West Antarctica, from 1992 to
505 2011, *Geophys. Res. Lett.*, **41**, 3502–3509, doi.org/10.1002/2014GL060140, 2014.
- 506 Rignot, E., Mouginot, J. and Scheuchl, B. MEaSURES Antarctic Grounding Line from Differential
507 Satellite Radar Interferometry, Version 2. [Indicate subset used]. Boulder, Colorado USA. NASA
508 National Snow and Ice Data Center Distributed Active Archive Center. doi:
509 <http://dx.doi.org/10.5067/IKBWW4RYHF1Q>, 2016.
- 510 Rignot, E., Mouginot, J. and Scheuchl, B. MEaSURES InSAR Based Antarctica Ice Velocity Map, Version
511 2. [Indicate subset used]. Boulder, Colorado USA. NASA National Snow and Ice Data Center
512 Distributed Active Archive Center. doi: <http://dx.doi.org/10.5067/D7GK8F5J8M8R>. [24th April
513 2017], 2017.
- 514 Rott, H., Rack, W., Nagler, T. and Skvarca, P. Climatically induced retreat and collapse of northern
515 Larsen Ice Shelf, Antarctic Peninsula, *Ann. Glaciol.*, **27**, 86–92, 1998.
- 516 Scambos, T.A., Hulbe, C., Fahnestock, M. and Bohlander, J. The link between climate warming and
517 break-up of ice shelves in the Antarctic Peninsula, *J. Glaciol.*, **46**, 516–530, 2000.
- 518 Scambos, T. A., Bohlander, J.A., Shuman, C. A. and Skvarca, P. Glacier acceleration and thinning after
519 ice shelf collapse in the Larsen B embayment, Antarctica, *Geophys. Res. Lett.*, **31**, L18402,
520 <https://doi.org/10.1029/2004GL020670>, 2004.
- 521 Scambos, T., Haran, T., Fahnestock, M., Painter, T. and Bohlander, J. MODIS-based Mosaic of
522 Antarctica (MOA) Data Sets: Continent-wide Surface Morphology and Snow Grain Size, *Remote
523 Sensing of Environment*, **111**(2): 242-257. <http://dx.doi.org/10.1016/j.rse.2006.12.020>, 2007.
- 524 Schaffer, J., Timmermann, R., Arndt, J. E., Kristensen, S. S., Mayer, C., Morlighem, M., and Steinhage,
525 D.: A global, high-resolution data set of ice sheet topography, cavity geometry, and ocean
526 bathymetry, *Earth Syst. Sci. Data*, **8**, 543-557, <https://doi.org/10.5194/essd-8-543-2016>, 2016.
- 527 Schannwell, C., Cornford, S., Pollard, D., and Barrand, N. E. Dynamic response of Antarctic Peninsula
528 Ice Sheet to potential collapse of Larsen C and George VI ice shelves, *The Cryosphere*, **12**, 2307-
529 2326, <https://doi.org/10.5194/tc-12-2307-2018>, 2018.
- 530 Seroussi, H., Morlighem, M., Rignot, E., Larour, E., Aubry, D., Dhia, H. and Kristensen, S.S. Ice flux
531 divergence anomalies on 79North Glacier, Greenland, *Geophysical Research Letters*, **38**, L09501,
532 [doi:10.1029/2011GL047338](https://doi.org/10.1029/2011GL047338), 2011.
- 533 Studinger, M. IceBridge ATM L2 Icessn Elevation, Slope, and Roughness, Version 2. [ILATM2_2010
534 and ILATM_2014]. Boulder, Colorado USA. NASA National Snow and Ice Data Center Distributed



- 535 Active Archive Center. doi: <https://doi.org/10.5067/CPRXXK3F39RV>. [Date Accessed: 2016], 2014,
536 updated 2018.
- 537 Walters, R., Josberger, E.G. and Driedger, C.L. Columbia Bay, Alaska: An upside down estuary.
538 Estuarine, Coastal and Shelf, *Science*, **26**, 607–617, 1988.
- 539 Wilson, N.J. and F. Straneo. 2015. Water exchange between the continental shelf and the cavity
540 beneath Nioghalvfjærdsbræ (79 North Glacier). *Geophysical Research Letters*,
541 10.1002/2015GL064944
- 542